Journal of Hydrology 410 (2011) 226–238

Contents lists available at SciVerse ScienceDirect

Journal of Hydrology

journal homepage: www.elsevier.com/locate/jhydrol

Effects of land cover on runoff coefficient

Nutchanart Sriwongsitanon *, Wisuwat Taesombat

Department of Water Resources Engineering, Faculty of Engineering, Kasetsart University, Bangkok 10900, Thailand

ARTICLE INFO

Article history:
Received 4 June 2010
Received in revised form 18 May 2011
Accepted 18 September 2011
Available online 29 September 2011
This manuscript was handled by Konstantine P. Georgakakos, Editor-in-Chief, with the assistance of V. Lakshmi, Associate Editor

Keywords:
Landsat 5 TM
Land cover
Flood hydrology
Runoff coefficient
Peak flood events
Upper Ping River Basin

SUMMARY

Land cover is considered to have significant influence on the hydrologic response of a river basin. In this study, we assessed how changes in land cover over time affected flood behaviour from 1988 to 2005, in the Upper Ping River Basin, northern Thailand. We correlated the types of land cover with rainfall–runoff behaviour for smaller and larger flood events taking place during this period. To quantify land cover, nine Landsat 5 TM images taken during the dry season (January or February) were obtained and processed to examine inter-annual land cover changes. From the networks of daily read rainfall data and stream gaugings available across the basin, 68 rainfall and 11 runoff stations were selected to evaluate peak flow rate and runoff coefficient for flood events. For individual sub-catchments, strong non-linear correlations were found between the overall runoff coefficient and peak flow rates for flood events. These runoff coefficients to peak flow relationships varied from year to year with different land cover for each sub-catchment. From these relationships within a particular sub-catchment, we determined relationships between different types of land cover and runoff coefficient for the 2, 5, 10 and 15 year Annual Recurrence Interval (ARI) peak flood events. We found that runoff coefficient increased with increasing forest proportion for these specified peak flood conditions, on nine out of eleven sub-catchments. On the other hand, the runoff coefficient associated with these peak flood events decreased as agricultural and disturbed forest areas increased. The influence of land cover on runoff coefficient was, however, found to be very different between smaller (lower than ~2 year ARI) and larger flood events (larger than ~2 year ARI). Runoff coefficient is higher for high forest cover during larger flood events; but for smaller flood events, runoff coefficient is lower when forest cover is high. This is due to the fact that for smaller flood events, rainfall loss rate for the forest area is normally higher than that of the non-forest area according to higher evapotranspiration and soil moisture capacity. Forests have proved to potentially offer flood mitigation benefits for smaller flood events. However, for larger flood events the situation of the basin can be different, especially on a basin with higher antecedent soil moisture or even under saturation stage. Antecedent soil moisture from the previous storms could be better retained within the forest area than the non-forest area due to deeper rote zone and higher soil moisture holding capacity of the forest area compared to non-forest area. For the larger flood events, forest area tends to produce more runoff than non-forest area as found in this study. These findings gave us a more thorough understanding of the effect of land cover types on flood behaviour at different stages of soil moisture conditions, and the severity of storm events. It can be useful for land use and flood management of the river basin.

1. Introduction

Internationally, there has been much concern for quite some time that deforestation of upland catchments may alter downstream flood hydrology. This concern has been fostered by the strong evidence that deforestation leads to increased flooding on scales smaller than 2 km^2 (Bosch and Hewlett, 1982). However, for larger catchments the situation is more complex. The limited numbers of studies that have quantified effects of land cover changes on flood behaviour report a diversity of results. Some studies reported that deforestation is linked with an increase in flood peaks and flood volumes (Bates and Henry, 1928; Fritsch, 1990; Lavabre et al., 1993), a number of other studies finding no definite change in flood behaviour (Hibbert, 1967; McGuinness and Harrold, 1971; Hewlett, 1982; Robinson et al., 1991; Beschta et al., 2000; Andréassian, 2004), and some studies even showing evidence that flooding reduces as deforestation occurs (Troendle and King, 1985; Hornbeck et al., 1997; Austin, 1999).

Lin and Wei (2008) provide a good example of a large scale study showing a trend of increased flooding with decreasing forest cover.

* Corresponding author. Address: Department of Water Resources Engineering, Faculty of Engineering, Kasetsart University, 50 Paholyothin Rd., Ladyao, Jatujak, Bangkok 10900, Thailand. Tel./fax: +66 2 5791567.
E-mail addresses: fengnns@ku.ac.th (N. Sriwongsitanon), fengwwt@ku.ac.th (W. Taesombat).

0022-1694/$ - see front matter © 2011 Elsevier B.V. All rights reserved.
doi:10.1016/j.jhydrol.2011.09.021

Their study was conducted in the Willow catchment (2860 km^2) in Canada. The majority of the catchment consists of a long, broad valley at low to medium elevations and gentle to moderate slopes. They showed evidence that deforestation in the catchment significantly increased mean and peak flows between 1957 and 2005 during spring periods; however, the mean and peak flows in summer and winter were not significantly affected. Legesse et al. (2003) also concluded – in their study on hydrological response of a catchment to climate and land use changes in south-central Ethiopia – that changing a catchment which is dominantly covered by cultivated/grazing land to woodland, would increase the evaporation loss and decrease mean annual discharge. More broadly, in a study based on a dataset of national statistics of land cover change and flood characteristics, Bradshaw et al. (2007) concluded that deforestation is strongly correlated with flood occurrence and severity. However, Van Dijk et al. (2009) re-examined this data set and concluded that the understanding of how deforestation impacts on hydrology for large scale catchments is far from complete. They went on to cite many recent studies on large-scale catchments that found no significant changes in hydrology even after deforestation of up to 50% of the catchment. Furthermore, they found that where changes did occur, these were not directly attributable to deforestation. Van Dijk et al. (2009) concluded that until now, there has not been convincing empirical evidence or theoretical argument that removal of trees is likely to increase severe flooding.

Case studies that showed flood flows on large-scale catchments were not significantly affected by land cover change include Buttle and Metcalfe (2000) who found only limited flow responses to land cover changes of 5–25%, for catchments in Northeastern Ontario, Canada, with no definitive changes in annual flood peak. Dyhr-Nielsen (1986) also concluded that there were no significant trends in streamflow in the Pasak River Basin in Central Thailand, where changes in forest cover of up to 50% were observed. Wilk et al. (2001) did not find any significant change in hydrological behaviour after deforestation in the Nam Pong River Basin in northeastern Thailand when forest cover declined from 80% in 1957 to 27% in 1995. Adamson (2005) also reported that there were no definitive changes in the observed river hydrology of the Mekong River Basin over the last 90 years, despite the significant land cover changes in the basin during that period.

Few studies have shown deforestation to be linked to a decrease in peak flows (Wei et al., 2008). A particularly significant study reported this trend was conducted on the Upper Penticton experimental basin in British Columbia, Canada (Austin, 1999).

After Andréassian (2004) carried out a thorough review on the paired-watershed experiments conducted throughout 20th century, he concluded that deforestation could definitely increase both flood volumes and flood peaks. However, this effect is much more variable than the effect on total flow and may even be inverted in some years or in some seasons. In some studies on reforestation, they show a very limited effect on floods in general, and no effect at all on the large ones. This corresponds to the conclusion made by Cosandey et al. (2005), who noted that the forest has a limited impact in the case of very heavy floods, whereas its effect has been confirmed when flood flows are lower. This is associated with the scientific perception which appreciates that forests generally evaporate more water than other land uses which tends to lead to a general reduction in catchment flows (Calder and Aylward, 2006). From theoretical considerations, it would be expected that interception of rainfall by forests reduces floods by removing a proportion of the storm rainfall, and by allowing the build up of soil moisture deficits, rather than leaving it to soak into the rivers and streams until the soil becomes saturated. After that, the water stops infiltrating into the soil and all of it flows into the waterways. When we have major floods, the soils become saturated early on; and once they are saturated it does not matter whether or not there is forest or any other types of land cover (Lull and Reinhart, 1972).

Until 30 years ago, the heterogeneous nature of land cover changes across large catchments made their accurate assessment difficult. However, remote sensing now provides an invaluable tool for accurately detecting land cover change.

Through this paper we seek to improve the understanding of land cover impacts on flood behaviour by analyzing data available for the Upper Ping River Basin (UPRB) by: (1) determining the land cover changes from 1988 to 2005 using the Landsat 5 TM satellite images, (2) calculating the runoff coefficient for runoff stations for monsoonal flood events within the same period, and (3) determining correlative relationships between different types of land cover and runoff coefficients for those flood events.

2. The study area

The Ping River is one of the main tributaries of the largest river basin within Thailand, the Chao Phraya, which drains more than one-third of the country's land area, making it Thailand's largest river basin. The Ping originates in the far north of Thailand in Chiang Dao District. From there it flows south through Chiang Mai City into the Bhumibol Reservoir, which has an active storage capacity of 9.7×10^9 m^3, as shown in Fig. 1. It is this portion above the Bhumibol Reservoir that is referred to as the UPRB.

With Thailand's economic development, there is increasing concern about land cover changes and flooding in the Chao Praya Basin. For example, between 25 and 30 September 2005, Typhoon Damrey devastated the UPRB, displacing 24395 people and causing around 100 million baht (3 million US dollars) of widespread economic damage across Chiang Mai Province (Department of Disaster Prevention and Mitigation, 2005).

The UPRB has an area of approximately 25370 km^2 and is located between 16°54′ and 19°51′N latitude, 97°48′ and 99°36′E longitude. The basin is dominated by well-forested, steep mountains in a generally north–south alignment. The average annual rainfall and runoff of the basin between 1988 and 2005 were 1174 mm and 268 mm, respectively (Taesombat and Sriwongsitanon, 2010). Eleven sub-catchments with the areas ranging between 240 and 3858 km^2 were used in the study and their average catchment area is around 1667 km^2.

Flooding is an issue of critical concern for water resources management in the UPRB. Floods on the UPRB occur annually due to heavy seasonal rains from both the south-west monsoon and tropical storms related to typhoon events in the South China Sea.

Historically, the UPRB was a heavily forested landscape, but by 2006 forest cover had declined to 72% (Royal Forest Department, 2006). Over the last 30–40 years, this deforestation on the UPRB has occurred due to agriculture and the expansion of urban communities. Much of this deforestation has been driven by economic development in and around Chiang Mai, a city of around 2 million people and northern Thailand's most important economic urban centre, which is located in the north-central area of the UPRB. There has been much speculation that deforestation has increased the risk of flooding on the Upper Ping and its tributaries; however, to date, few studies have directly addressed the links between changing land cover and flooding in the UPRB, in a rigorous manner.

3. Data collection and catchment characterizations

Relationships between different types of land cover and runoff coefficients for the UPRB were investigated in this study using TM satellite images, as well as rainfall and runoff data, during the same period. Details of data used are described below.

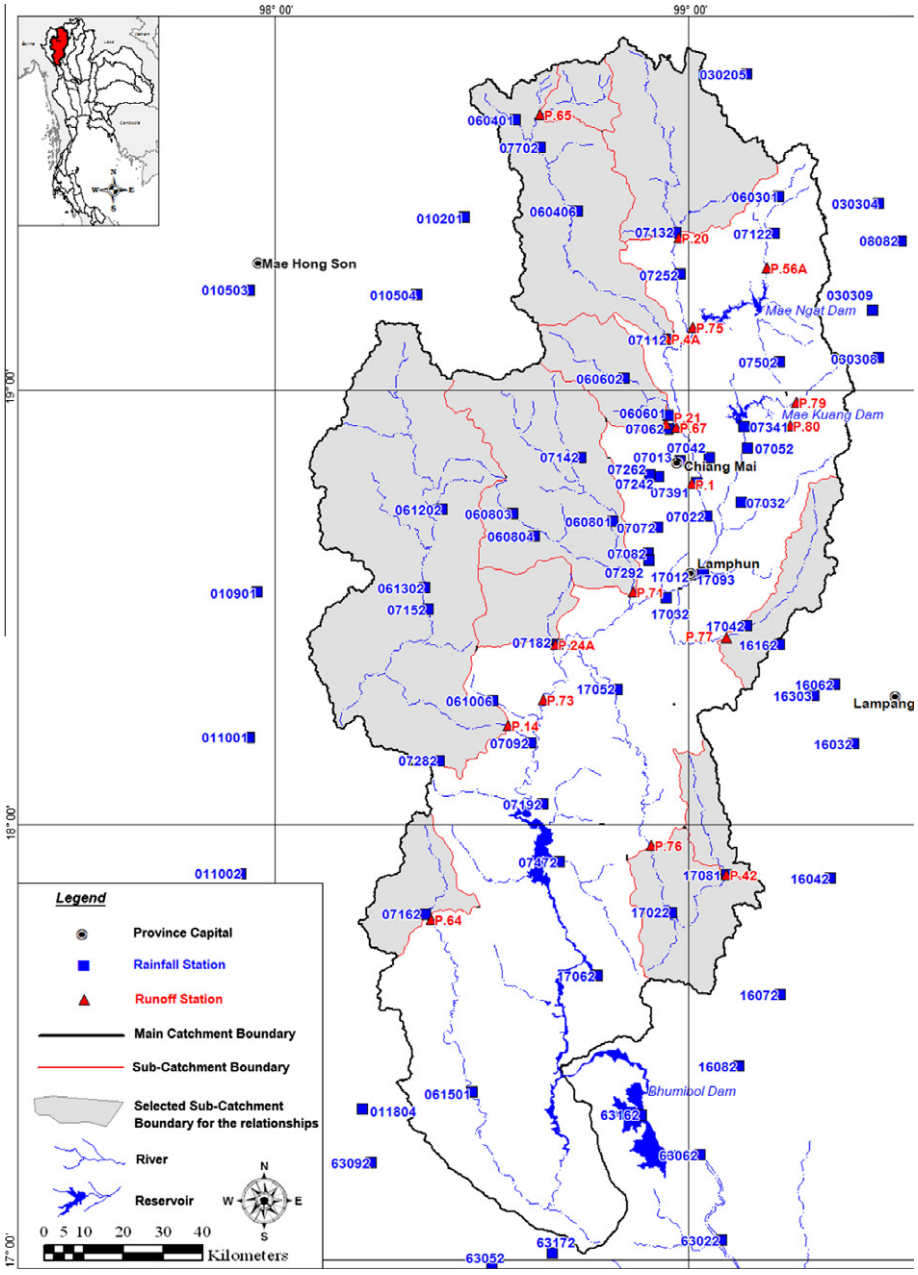

Fig. 1. Sub-catchments and locations of rainfall and runoff stations in the UPRB.

3.1. TM satellite images

Nine TM satellite images of the UPRB located on path 131, row 46, 47, and 48 were used for land cover classification. These images were obtained for the years 1988, 1993, 1994, 1995, 1996, 2000, 2001, 2002, and 2005 from the Geo-Informatics and Space Technology Development Agency (GISTDA) of Thailand. Conditions were cloud-free over the basin for seven images and had less than 1% cloud cover for two images taken in 1994 and 1996. All images were taken in the mid-dry season (January–February) to reduce possible influences of seasonal changes in soil and vegetation conditions.

3.2. Daily rainfall data

Daily rainfall readings were available from a network of 68 stations within the UPRB operated by the Royal Irrigation Department (RID), the Thai Meteorology Department (TMD) and the Department of Water Resources (DWR) at locations as shown in Fig. 1. From these daily readings, areal rainfall distributions across the UPRB were generated using the Thin Plate Spline (TPS) for the years between 1988 and 2005 when the nine TM satellite images were available. The TPS technique was used in this study because it was proved to provide more accurate results of rainfall estimation than those of given by two conventional techniques, the Isohyetal and Thiessen polygon techniques. Further details on the rainfall data and generation of areal rainfall distributions are provided in Taesombat and Sriwongsitanon (2009).

3.3. Daily runoff data

RID operates 18 daily read runoff stations in the UPRB at the locations shown in Fig. 1. Data at these stations were used to determine peak and nett runoff for selected flood events for the years

Table 1
Catchment characteristics and summary of hydrologic conditions for selected sub-catchments in the UPRB. *Source*: Taesombat and Sriwongsitanon (2010).

Sub-catchment	P.4A	P.14	P.20	P.21	P.24A	P.42	P.64	P.65	P.71	P.76	P.77
Area (km^2)	1902	3853	1355	515	460	315	336	240	1771	1541	547
Altitude range (m)	1020	991	790	731	888	672	1090	1122	828	618	641
Average channel slope (%)	0.78	0.81	0.80	0.72	0.98	0.42	0.49	0.64	0.69	0.41	0.63
Number of years data is coincident with land cover data	9	9	9	9	9	6	8	8	5	4	4
Average rainfall (mm/yr)	1142	1128	1023	1029	1043	862	1056	1162	1088	828	922
Average runoff (mm/yr)	187	258	277	229	290	103	434	508	161	130	146
%Runoff	16.4	22.8	27.1	22.3	27.8	12.0	41.1	43.7	14.8	15.7	15.8

between 1988 and 2005, when satellite images were available. However, data from a number of these stations were unsuitable for use in the study as:

1. data from station P.56A can be affected by backwater from the Mae Ngat reservoir so readings from this station could be unreliable, especially during flood events;
2. stations P.75, P.67, P.1 and P.73 were not used as they are downstream of the Mae Ngat and Mae Kuang Reservoirs, so reservoir operations would be expected to affect flood behaviour at these stations;
3. data collection at stations P.79 and P.80 only commenced in 2001, so data were only presented for the 2001, 2002 and 2005 satellite data events.

With these stations omitted, Table 1 summarizes the features of the 11 remaining stations and their associated sub-catchments that were used in the analysis.

Data availability was generally very good with 5 stations having data coincident with all 9 years when images were obtained. The other 6 stations started operating through the period of the study, with 2 of the stations having 8 years of data and the remaining stations having 4–6 years of data available.

Topographic data to delineate sub-catchments was obtained from Taesombat and Sriwongsitanon (2010). As can be seen in Table 1, the sub-catchments above the stream gauging stations ranged in size from 240 to 3853 km^2, with a cluster of 6 smaller sub-catchments ranging from 240 to 547 km^2, a cluster of medium sized sub-catchments between 1355 and 1902 km^2, and one large catchment (3853 km^2). All catchments were generally mountainous with altitude ranges between 641 and 1020 m.

4. Methodology

4.1. Remote sensing analysis for producing a land cover map

4.1.1. Geometric correction

Geometric correction aims to remove geometric distortions introduced by a variety of factors which vary for each image acquisition event to ensure individual picture pixels are placed in their proper planimetric map locations (Sriwongsiatnon et al., 2011). Nine predominately cloud-free TM satellite images of the UPRB were referenced to the Universal Transverse Mercator (UTM) Zone 47N geographic projection using the World Geodetic System 1984 (WGS 84). The 1:50000 scale topographic map (L7018) prepared by the Royal Thai Survey Department (RTSD) was used for image rectification. Image-to-map rectification was applied to the first image taken in 2005 using 40 well distributed ground control points (GCPs) in the reference process. Image-to-image rectification was used for the other eight images. A nearest-neighbour resampling scheme was used to preserve the original brightness values of the images.

4.1.2. Radiometric correction

After geometric correction, those 9 satellite images of the UPRB were processed by radiometric correction. This procedure aims to transform image data from multiple sensors and platforms into a common radiometric scale and reduces signal variations unrelated to the brightness of the image surface, such as spectral radiance and top-of-atmospheric reflectance. Images taken on different dates and/or by different sensors can be directly compared after applying radiometric correction (Sriwongsiatnon et al., 2011). Spectral information from TM imagery is in the format of a Digital Number (DN). At-sensor spectral radiance (L) in $W\,m^{-2}\,sr^{-1}\,\mu m^{-1}$ can be calculated from the remotely sensed DN values using following equation,

$$L = G(DN) + B \tag{1}$$

where G is the band-specific rescaling gain factor and B is the band-specific rescaling bias factor. The current parameter values for radiometric correction for Landsat 5 as used here were evaluated by Chander et al. (2007).

The spectral radiance calculated using Eq. (1) was converted to a planetary or exoatmospheric reflectance, calculated by Eq. (2), to reduce variability between scenes for better image comparison. This process can remove the cosine effect of different solar zenith angles arising from different acquisition time and can compensate for different values of the exoatmospheric solar radiances due to spectral band differences (Chander and Markham, 2003),

$$R^* = \frac{\pi d^2 L}{E_0 \cos\theta_z} \tag{2}$$

where R^* is the top of atmospheric (TOA) reflectance (unitless), d is the earth–sun distance in astronomical units, E_0 is the mean solar exoatmospheric spectral irradiance (data values were evaluated by Chander and Markham (2003)), and θ_z is the solar zenith angle (degrees). The earth–sun distance (d) has a relationship to the Julian day (Dy) of the satellite data acquisition as shown in following equation.

$$d = 1 - [0.01672\cos(0.9856(Dy - 4))] \tag{3}$$

4.1.3. Land cover classification

The nine post-processing satellite images were used for land cover classification. The colour composite image of Landsat 5 TM bands 4-5-3 which were assigned as red, green, and blue, respectively were selected to classify the land cover across the UPRB. This is due to Scepan et al. (1999), who suggested that these bands combination are one of the most useful band combinations in Landsat for discrimination of land cover categories. Unsupervised classification by K-means algorithm was applied to all bands (except the thermal band) to categorize the different major land cover types. We first worked on the image taken in 2000 when the Land Development Department performed ground data collection on the UPRB. The major land cover types distinguished by unsupervised classification were compared to the ground truth data to separate land cover types into 5 categories consisting of forest, disturbed forest, agricultural areas, water bodies and urban areas. Supervised classification was later applied to all 6 bands by identifying the ROI (region of interest) of these 5 land cover types. These ROIs were used to automatically classify land cover types for the whole basin

using parallelepiped with maximum likelihood classifier. Since the maximum likelihood classifier was applied, atmospheric correction is not a necessary step to carry out (Song et al., 2001). As long as the training data and the image to be classified are on the same relative scale, atmospheric correction has little effect on classification accuracy (Potter, 1974; Fraser et al., 1977; Kawata et al., 1990).

We also conducted a ground truth survey from March 28 to April 10, 2007, across the UPRB to check the results of land cover classification. Because of the delay in time between the ground truth survey and the studied satellite images, particular attention was paid to verifying land cover at locations where land cover changes were unlikely, such as remote forest areas, and well established agricultural and urban areas. Results of the verification confirmed the classification results, so classification could then be applied, with confidence, to the other 8 Landsat 5 TM images, to determine land cover across the UPRB from 1988 to 2005.

4.2. Investigation of the relationship between different types of land cover and flood characteristics

Analyzing how land cover change impacts on flood events on each sub-catchment involved firstly determining the peak flow rate and the proportion of runoff to rainfall (runoff coefficient) associated with flood events for years during the study period, when Landsat 5 TM data were available. Correlation relationships between runoff coefficients and peak flow rates were then determined over the whole study period and from 1 year to the next for each sub-catchment. Next, runoff coefficients corresponding to peak flood events of 2, 5, 10 and 15 year Annual Recurrence Interval (ARI), as well as to peak flood events of less than 2 year ARI, were determined from the correlations for each year of the study period on each of the 11 sub-catchments. These peak flows were then correlated against the observed land cover. Details for each of these steps are discussed below.

4.2.1. Determination of runoff coefficients for flood events

Determination of the runoff coefficients for flood events on each sub-catchment was performed using standard flood analysis techniques on events with single peaked hydrographs in two steps:

1. Baseflow was removed from the flood hydrograph, as it represents the contribution from antecedent precipitation, rather than from the immediate event. This was done by constructing a trapezoid between the minimum flow points at the start and end of the event. Runoff coefficient was then calculated as the area under the hydrograph divided by the sub-catchment area and the rainfall. (Note that no adjustments were made to peak flow rates.)
2. Rainfall related to a particular flood event was included when the discharge started to rise at the start of the event, until it started to fall at the end of the event.

4.2.2. Relationships between runoff coefficients and peak flow rates for larger flood events

Runoff coefficient is widely used as a diagnostic variable to represent runoff generation in a catchment and as an important input parameter in hydrologic design. Merz et al. (2006) calculated the runoff coefficients for 50000 events in 337 Austrian catchments with catchment areas ranging from 80 to 10000 km^2 over the period 1981–2000. They concluded that runoff coefficients are controlled by the climate and the runoff regime through the seasonal catchment water balance, and hence antecedent soil moisture is added to event characteristics. The driest catchment has the smallest runoff coefficients while the wettest catchment has the largest runoff coefficients. The large runoff coefficients were caused by an

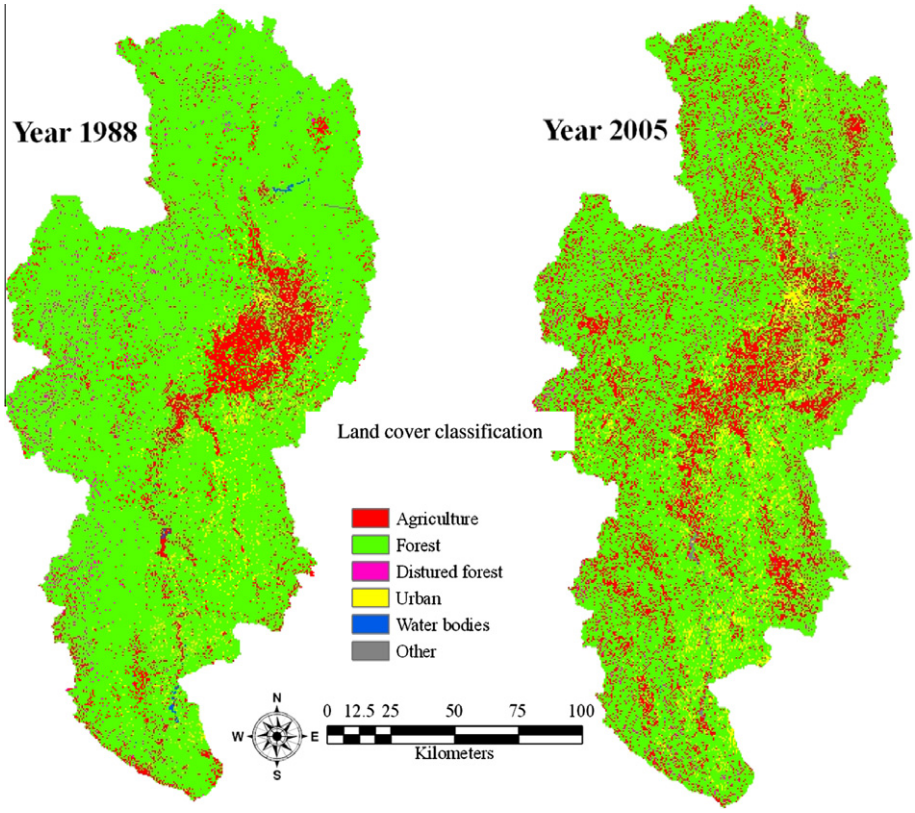

Fig. 2. Land cover for the UPRB from Landsat 5 TM in 1988 and 2005.

increase of antecedent soil moisture due to snowmelt and rain falling on wet soils. According to this finding, we correlated the peak flow rates, which is also an important parameter that can be used to define the magnitude of a given flow event, with runoff coefficients, based on the assumption that these two parameters would normally be displayed as well correlated.

With this in mind, we firstly checked that runoff coefficients and peak flow rates were overall well correlated for each sub-catchment. Next we determined the correlation relationships between runoff coefficients and peak flow rates for each sub-catchment on a year by year basis, to see if these relationships were changing over time.

We then looked for evidence that the runoff coefficients to peak flow relationships were related to land cover types. Our primary interest here is in flood event; however, we only had limited data available, so we compromised by considering how flood hydrology might be affected by land cover for the 2, 5, 10 and 15 year ARI peak flows events (as determined by Log Pearson III, statistics over the length of records available, 1954 to 2006 for most sub-catchments). Despite the fact that the premise of stationarity for the proper use of the LP3 methodology cannot be guaranteed in the present study, due to the changes in the land cover of the basins, we have used the methodology as a proxy for estimating the different ARI values. We applied these peak flow values to the runoff coefficients for the 9 peak flow regression relationships relevant to each year, in the study period for each of the 11 sub-catchments, to determine a set of 297 runoff coefficients that corresponded to particular ARI flow rates. We then determined how these runoff coefficients were correlated with different types of land cover comprising percentage forest areas, deforested areas, agricultural areas, and urban areas for each sub-catchment. Under this approach, once runoff coefficients and different types land cover were found to be correlated, we can have some confidence that change in streamflow is related to change in land cover.

4.3. Relationships between runoff coefficients and land cover for smaller flood events

We realized in the previous section that the relationships between runoff coefficients and peak flow rates for larger flood events (larger than around 2 year ARI) would differ from the relationships for smaller flood events (less than approximately 2 year ARI). These differences would possibly depend on different antecedent soil moisture condition of the catchment between smaller and larger flood events. The relationships between runoff coefficients and different types of land cover for smaller flood events were later investigated, on the same 11 selected sub-catchments, to see how effects on runoff coefficients and land cover. For smaller

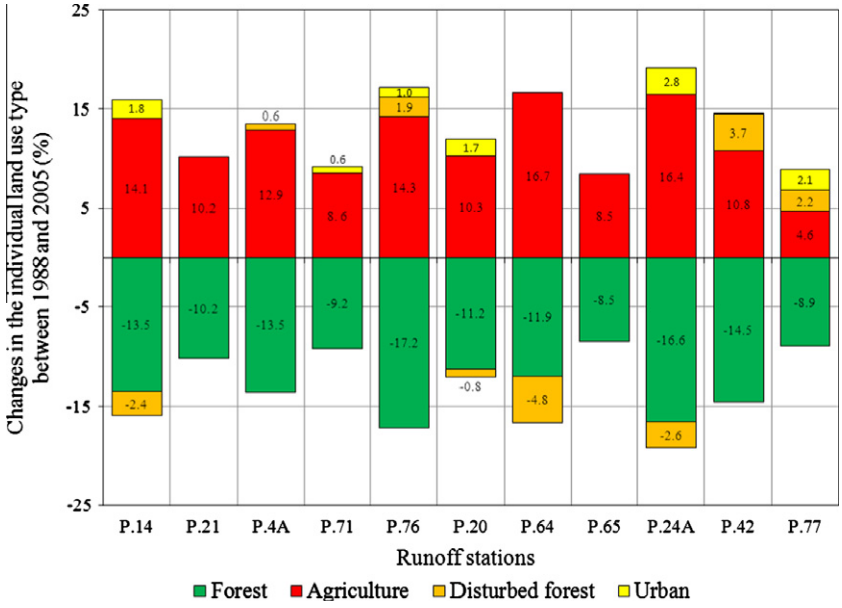

Fig. 3. Changes in land cover for the selected sub-catchments in the UPRB between 1988 and 2005.

Table 2
Correlations of runoff coefficients (C) and peak flow rates (Q_P) for selected sub-catchments in the UPRB.

Runoff station	No. of selected flood events	Range of peak (yr ARI)	$C = a\,(Q_p)^b$			$C = a\,(Q_p/A)^b$		
			a	b	r	a	b	r
P.4A	30	~1–15	0.0228	0.39	0.74	0.4219	0.39	0.74
P.14	67	~1–10	0.0009	0.91	0.78	1.6256	0.91	0.78
P.20	56	~1–86	0.0036	0.87	0.86	1.8918	0.87	0.86
P.21	49	~1–15	0.0181	0.63	0.74	0.9126	0.63	0.74
P.24A	29	~1–6	0.0133	0.77	0.79	1.4903	0.77	0.79
P.42	28	~1–2	0.0177	0.83	0.91	2.0492	0.83	0.91
P.64	48	~1–4	0.0124	0.85	0.76	1.5606	0.81	0.76
P.65	43	~1–10	0.0110	0.90	0.93	1.5178	0.90	0.93
P.71	31	~1–16	0.0058	0.75	0.89	1.1247	0.71	0.89
P.76	20	~1–11	0.0057	0.71	0.89	1.4714	0.75	0.89
P.77	25	~1–4	0.0165	0.71	0.81	1.4105	0.72	0.81

flood events, the catchment would have low antecedent soil moisture, so this would make an interesting comparison with the result from the previous section.

For all runoff data within 9 years between 1988 and 2005, we selected all smaller flood events during the monsoonal period from May to October (6 months), except larger flood events which were analyzed within the previous section. For these flood hydrographs, we considered the volume of rainfall and runoff (with base flow removed) in order to determine the runoff coefficient, and then the correlation between runoff coefficients and land cover under low antecedent soil moisture conditions. We then determined runoff coefficient for this period on each of the 11 sub-catchments and correlated these against the observed forest area and agriculture plus disturbed forest in each year.

5. Results and discussion

5.1. Land cover classification

General land cover trends for the UPRB are shown in Figs. 2 and 3. Note in particular that forest cover across the UPRB was generally decreasing from 21833 km^2 (86.1% of the total catchment area) in 1988 to 19149 km^2 (75.5%) in 2005. Conversely, areas under agricultural, urbanized, and water bodies increased from 9.5%, 2.6% and 0.1% of the total catchment area in 1988 to 18.3%, 4.7% and 0.3%, respectively in 2005, while disturbed forest areas decreased from 1.7% in 1988 to 1.3% in 2005.

5.2. Correlations between runoff coefficients and land cover for larger flood events

Non-linear correlations that were well-fitted by power relationships were found between runoff coefficients and peak flow rates (~1–86 year ARI) for individual sub-catchment as shown in Table 2, with one example plotted in Fig. 4 for sub-catchment P.4A. The coefficient of correlation (r) for these relationships varied between 0.74 and 0.93, and the average was around 0.83. The values of the power parameter (b) of each sub-catchment varied between 0.39 and 0.91, while the multiplier, parameter (a) significantly varied from 0.0009 to 0.0228. Peak flow scales strongly related to the sub-catchment area, so we divided peak flows by sub-catchment area as shown in Table 2. The range of parameter (a) value narrowed to be between 0.4219 and 2.0492 across the sub-catchments.

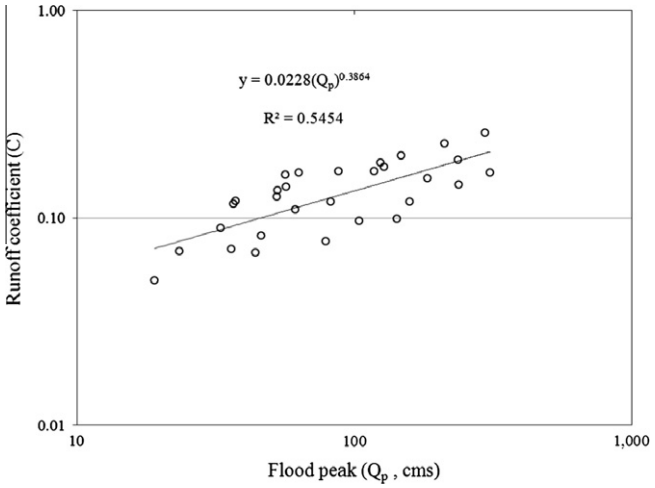

Fig. 4. Example of typical relationships between the runoff coefficients and peak flow rates for P.4A sub-catchment.

Table 3
Relationships between runoff coefficients (C) and peak flow rates (Q_P) for selected sub-catchments in the UPRB.

Runoff station	Area (km^2)	Non-linear regression $C = a\,(Q_p/A)^b$			
		Range of a	Range of b	r	
				Range	Average
P.65	240	1.04–8.94	0.79–1.37	0.84–0.99	0.92
P.42	315	1.23–350.00	0.66–2.34	0.91–0.99	0.96
P.64	336	0.84–255.44	0.46–2.81	0.65–0.99	0.88
P.24A	460	1.10–12.81	0.68–2.19	0.79–0.99	0.87
P.21	515	0.33–22.21	0.29–1.81	0.73–0.98	0.86
P.77	547	0.66–2.68	0.50–0.91	0.84–0.88	0.86
P.20	1355	1.09–7.70	0.50–1.39	0.82–0.99	0.89
P.76	1541	0.76–14.89	0.61–1.29	0.91–0.97	0.94
P.71	1771	1.05–1.88	0.67–0.81	0.75–0.99	0.83
P.4A	1902	0.51–1.33	0.40–0.72	0.69–0.89	0.80
P.14	3853	0.44–4.91	0.51–1.23	0.72–0.97	0.89
				Average	0.88

These runoff coefficient to peak flow relationships varied from year to year on each sub-catchment, as shown in Table 3. For each year in which land cover data was available, there was generally a distinct non-linear correlation relationship between runoff coefficients and flood peaks. The r coefficients varied from 0.80 to 0.96, and the average value was 0.88. A typical example of these correlations is plotted in Fig. 5 for sub-catchment P.4A.

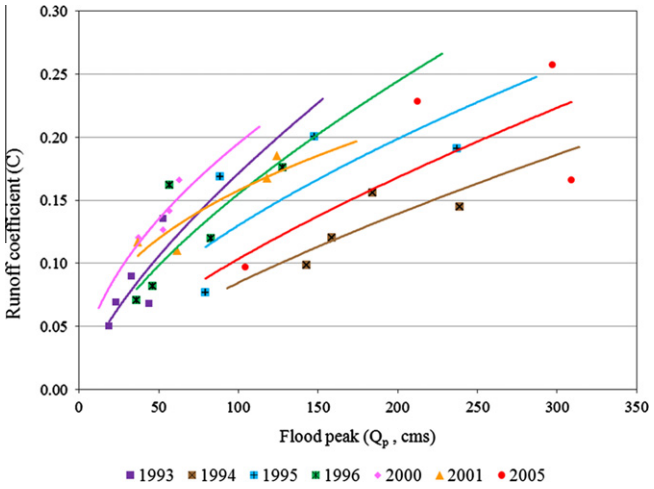

Fig. 5. Example of interannual relationships between runoff coefficients and flood peaks for P.4A sub-catchment.

Table 4
Flood peaks of ARI standardized events for selected sub-catchments in the UPRB.

Runoff station	Area (km^2)	Flood peak per area (cms/km^2)			
		2 years ARI	5 years ARI	10 years ARI	15 years ARI
P.65	240	0.13	0.20	0.25	0.27
P.42	315	0.09	0.13	0.16	0.17
P.64	336	0.25	0.41	0.51	0.54
P.24A	460	0.16	0.24	0.30	0.63
P.21	515	0.09	0.11	0.13	0.14
P.77	547	0.14	0.26	0.35	0.39
P.20	1355	0.09	0.15	0.20	0.22
P.76	1541	0.07	0.14	0.20	0.23
P.71	1771	0.09	0.11	0.13	0.13
P.4A	1902	0.07	0.11	0.15	0.16
P.14	3853	0.07	0.11	0.14	0.15

Table 5
Relationships between runoff coefficients (C) and land cover for larger flood events in the UPRB.

Runoff station	Given flood peak (years)	Forest area $C = a + b\,(F)$			Disturbed forest area $C = a + b\,(DF)$			Agricultural area $C = a + b\,(Ag)$			$DF + Ag$ area $C = a + b\,(DF + Ag)$		
		a	b	r	a	b	r	a	b	r	a	b	r
P.4A	2	−0.18	0.0042	0.62	0.17	−0.0006	0.09	0.19	−0.0034	0.50	0.23	−0.0041	0.59
	5	−0.26	0.0058	0.68	0.23	−0.0013	0.14	0.25	−0.0044	0.51	0.32	−0.0057	0.65
	10	−0.31	0.0069	0.69	0.28	−0.0018	0.17	0.30	−0.0050	0.50	0.38	−0.0069	0.67
	15	−0.34	0.0075	0.69	0.30	−0.0020	0.18	0.33	−0.0054	0.49	0.41	−0.0075	0.67
Average				0.67			0.14			0.50			0.65
P.14	2	−0.12	0.0033	0.69	0.16	−0.0011	0.22	0.17	−0.0021	0.44	0.20	−0.0032	0.66
	5	−0.36	0.0071	0.68	0.25	−0.0027	0.24	0.26	−0.0041	0.40	0.34	−0.0068	0.64
	10	−0.56	0.0102	0.67	0.32	−0.0041	0.26	0.33	−0.0057	0.37	0.45	−0.0099	0.63
	15	−0.66	0.0118	0.67	0.35	−0.0049	0.26	0.36	−0.0065	0.36	0.50	−0.0114	0.63
Average				0.68			0.25			0.39			0.64
P.20	2	−0.45	0.0080	0.67	0.29	−0.0110	0.41	0.31	−0.0085	0.53	0.40	−0.0135	0.81
	5	−1.25	0.0193	0.94	0.44	−0.0025	0.05	0.59	−0.0219	0.80	0.70	−0.0250	0.87
	10	−2.00	0.0295	0.91	0.55	0.0091	0.12	0.82	−0.0350	0.81	0.95	−0.0349	0.77
	15	−2.38	0.0347	0.88	0.59	0.0158	0.18	0.94	−0.0419	0.80	1.08	−0.0399	0.73
Average				0.85	0.47	0.0029	0.19	0.67	−0.0268	0.74	0.78	−0.0283	0.80
P.21	2	−1.22	0.0173	0.80	0.34	−0.0199	0.48	0.42	−0.0181	0.64	0.47	−0.0163	0.75
	5	−1.97	0.0272	0.76	0.50	−0.0337	0.49	0.61	−0.0282	0.60	0.71	−0.0261	0.72
	10	−2.49	0.0339	0.74	0.61	−0.0433	0.49	0.74	−0.0351	0.58	0.86	−0.0328	0.71
	15	−2.70	0.0367	0.73	0.65	−0.0473	0.49	0.79	−0.0379	0.57	0.93	−0.0357	0.70
Average				0.76			0.49			0.60			0.72
P.24A	2	0.99	−0.0079	0.66	0.29	0.0188	0.81	0.28	0.0063	0.42	0.18	0.0104	0.81
	5	1.31	−0.0091	0.56	0.48	0.0255	0.80	0.51	0.0054	0.26	0.37	0.0117	0.67
	10	1.37	−0.0077	0.29	0.64	0.0280	0.54	0.74	0.0015	0.05	0.58	0.0097	0.34
	15	1.34	−0.0063	0.19	0.72	0.0285	0.44	0.86	−0.0011	0.03	0.70	0.0079	0.22
Average				0.42			0.65			0.19			0.51
P.42	2	0.77	−0.0057	0.43	0.25	0.0047	0.42	0.28	−0.0016	0.10	0.21	0.0056	0.41
	5	1.18	−0.0090	0.41	0.35	0.0069	0.37	0.40	−0.0013	0.05	0.28	0.0089	0.40
	10	1.42	−0.0110	0.40	0.41	0.0082	0.36	0.46	−0.0011	0.03	0.32	0.0109	0.40
	15	1.52	−0.0118	0.40	0.43	0.0088	0.35	0.49	−0.0010	0.03	0.34	0.0117	0.39
Average				0.41			0.37			0.05			0.40
P.64	2	−10.21	0.1420	0.64	1.93	−0.0583	0.30	1.92	−0.0938	0.36	3.99	−0.1420	0.64
	5	−43.46	0.5854	0.65	6.77	−0.2564	0.32	6.31	−0.3572	0.33	15.08	−0.5854	0.65
	10	−80.50	1.0772	0.65	12.01	−0.4787	0.33	10.99	−0.6448	0.33	27.22	−1.0772	0.65
	15	−98.72	1.3188	0.65	14.58	−0.5883	0.33	13.27	−0.7855	0.33	33.16	−1.3188	0.65
Average				0.65			0.32			0.34			0.65
P.65	2	0.65	0.0104	0.47	0.29	−0.0017	0.10	0.33	−0.0149	0.48	0.39	−0.0104	0.47
	5	−1.50	0.0220	0.49	0.50	−0.0050	0.14	0.56	−0.0267	0.43	0.70	−0.0220	0.49
	10	−2.23	0.0317	0.50	0.65	−0.0081	0.16	0.73	−0.0360	0.41	0.94	−0.0317	0.50
	15	−2.58	0.0363	0.50	0.73	−0.0095	0.17	0.80	−0.0403	0.40	1.05	−0.0363	0.50
Average				0.49			0.14			0.43			0.49
P.71	2	−0.12	0.0041	0.75	0.24	−0.0023	0.25	0.29	−0.0069	0.85	0.28	−0.0039	0.71
	5	−0.15	0.0051	0.72	0.29	−0.0030	0.25	0.36	−0.0084	0.80	0.35	−0.0047	0.68
	10	−0.17	0.0055	0.70	0.31	−0.0033	0.25	0.39	−0.0090	0.78	0.37	−0.0051	0.66
	15	−0.17	0.0057	0.70	0.32	−0.0034	0.25	0.40	−0.0093	0.77	0.38	−0.0052	0.66
Average				0.72			0.25			0.80			0.68
P.76	2	−0.89	0.0153	0.72	0.34	−0.0138	0.54	0.24	0.0008	0.04	0.86	−0.0288	0.75
	5	−2.38	0.0388	0.63	0.78	−0.0431	0.58	0.41	0.0074	0.12	2.09	−0.0742	0.66
	10	−3.77	0.0604	0.59	1.18	−0.0722	0.59	0.52	0.0150	0.15	3.20	−0.1161	0.63
	15	−4.47	0.0714	0.58	1.38	−0.0873	0.60	0.57	0.0192	0.16	3.76	−0.1372	0.62
Average				0.63			0.58			0.11			0.67
P.77	2	−0.38	0.0085	0.67	0.35	−0.0027	0.17	0.45	−0.0146	0.76	0.48	−0.0101	0.71
	5	−1.33	0.0219	0.79	0.59	−0.0106	0.30	0.79	−0.0319	0.76	0.89	−0.0256	0.82
	10	−2.08	0.0323	0.82	0.76	−0.0171	0.34	1.02	−0.0447	0.75	1.19	−0.0376	0.85
	15	−2.42	0.0369	0.83	0.83	−0.0201	0.35	1.12	−0.0503	0.75	1.32	−0.0429	0.86
Average				0.78			0.29			0.75			0.81
Overall Average				0.64			0.33			0.45			0.64

The peak flows for the 2, 5, 10 and 15 year ARI events on each catchment are shown in Table 4. Using the correlation relationships reported in Table 3, runoff coefficients for these 2, 5, 10 and 15 year ARI events on each sub-catchment were determined and correlated against the proportion of forest area (*F*), disturbed forest area (*DF*), agricultural area (*Ag*) and the combined area of disturbed forest plus agricultural area (*DF* + *Ag*) on each sub-catchment as shown in Table 5. Two examples of the correlations between runoff coefficients and the proportion of forest area (*F*), as well as the combined area of disturbed forest plus agriculture (*DF* + *Ag*) are plotted for P.4A and P.21 in Figs. 6 and 7, respectively. Note that urban areas and areas of water bodies on the sub-catchments changed by such small amounts that they were not considered for this study.

Table 5 shows that linear correlation relationships were generally obtained between runoff coefficients and land cover. The relationships between runoff coefficients and forest area almost universally have positive slope (exponent "*b*" values were positive) for all of the sub-catchments except P.24A and P.42 (nine out of eleven sub-catchments). A positive slope on these correlations means that the runoff coefficient increases with increasing forest proportion for a particular peak flow event on each sub-catchment. The *b* values also tended to increase with an increasing return period of flood peaks for those nine sub-catchments. The average *r*

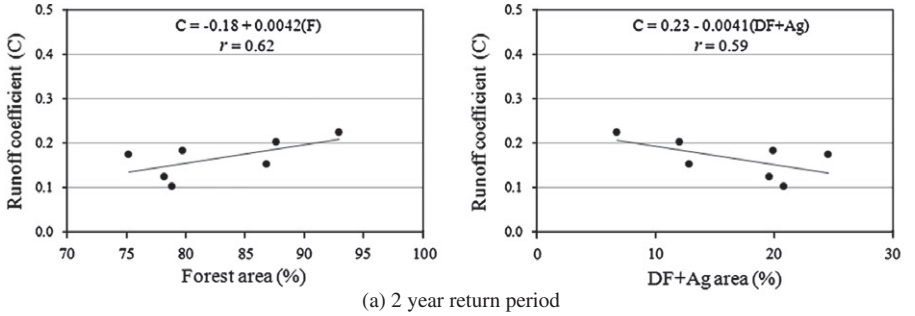

(a) 2 year return period

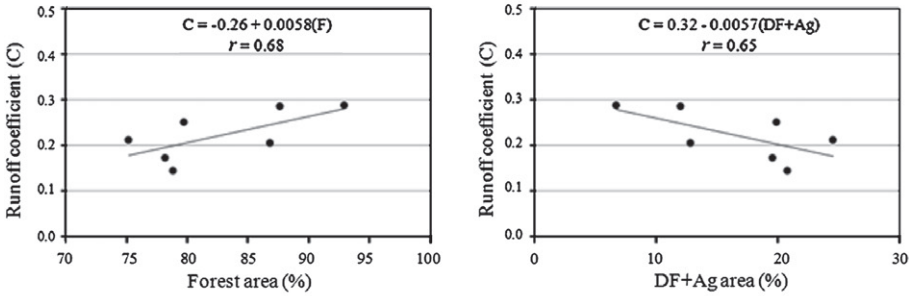

(b) 5 year return period

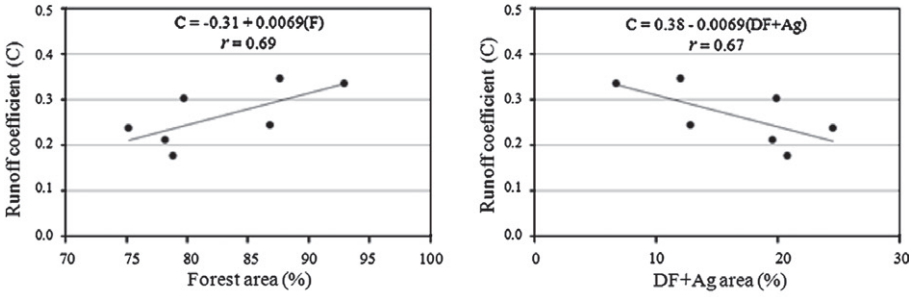

(c) 10 year return period

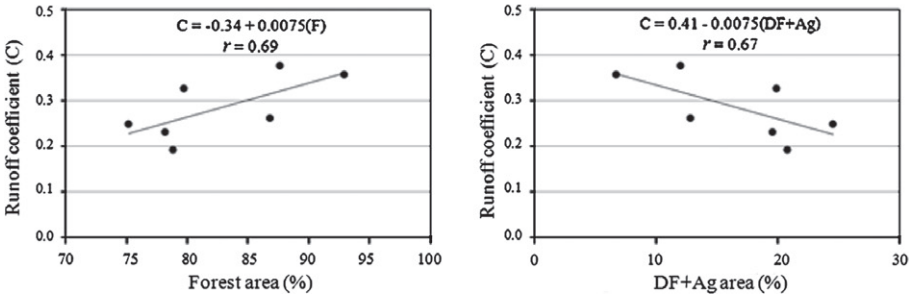

(d) 15 year return period

Fig. 6. Relationships between runoff coefficients and land cover for larger flood events for P.4A sub-catchment.

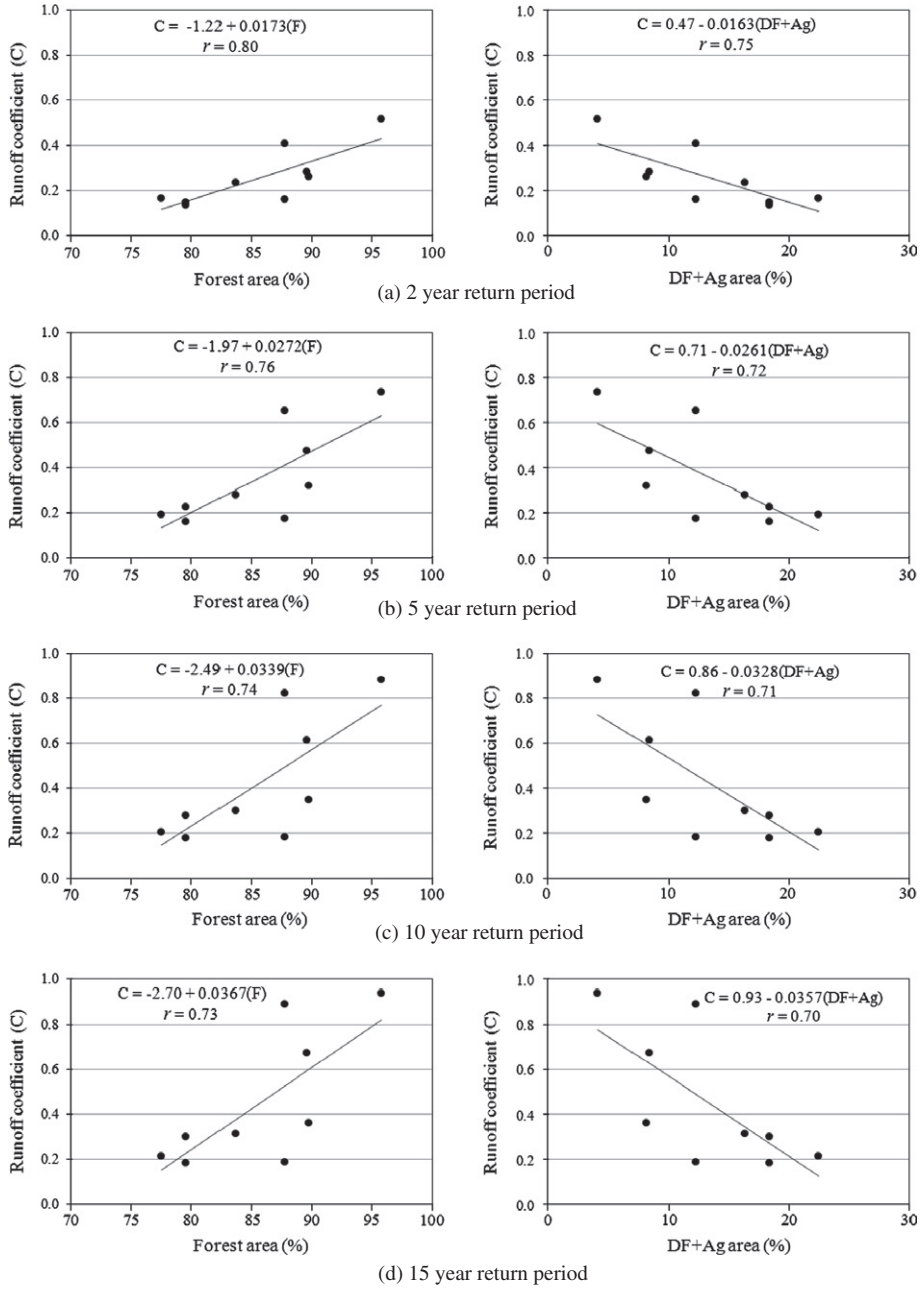

Fig. 7. Relationships between runoff coefficients and land cover for larger flood events for P.21 sub-catchment.

coefficient was around 0.64. Even for runoff stations with low *r*, all stations still show a positive slope, except P.24A and P.42. A higher proportion of forest on a catchment area was found to bring a higher proportion of runoff coefficient for a flood event.

Table 5 also shows that the relationships between runoff coefficients and the proportion of disturbed forest on the sub-catchment have a negative slope (*b* values were negative) for most of the sub-catchments. A similar result was found when runoff coefficients were correlated against the proportion of agricultural areas on the sub-catchments. The average *r* coefficients for both cases were around 0.33 and 0.45, respectively, which were quite low, but they still showed the same negative trend. We calculated the relationships between runoff coefficients and the combined area of disturbed forest plus agriculture. The relationships between the runoff coefficients and disturbed forests plus agriculture showed a negative slope (*b* values were negative) for most of the catchments except P.24A and P.42. The average *r* coefficients for these relationships increased compared to individual cases with the average value of around 0.64. The *b* values also tended to increase with an increasing return period of flood peaks for those sub-catchments, so we can see that when land cover changes, runoff coefficient decreases with increasing disturbed forest plus agricultural proportion on each sub-catchment. The more disturbed forest plus agricultural proportion will bring less runoff percentage over the same rainfall depth (lower runoff coefficient) at a particular flood peak flow.

Generally, the forest catchment generates more evapotranspiration, and so there is a greater soil moisture deficit and a lower discharge than the non-forest catchment (Bathurst et al., 2011). Forests may therefore reduce floods from small to moderate storms. However, there is growing evidence that this effect is increasingly reduced as rainfall increases to more extreme levels

(Beschta et al., 2000; Sikka et al., 2003; López-Moreno et al., 2006). This is according to antecedent conditions which affect basin storage capacity and hydraulic conductivity of soils (Kung et al., 2000; Buttle et al., 2001; Uhlenbrook, 2006). During dry periods, the storage capacity of the catchment is high and a substantial proportion of precipitation falling on the catchment is expected to be retained by storage. Under wetter conditions, the water table is elevated and the storage capacity of the catchment is reduced and the hydraulic conductivity of soil increases, causing increased runoff through upper soil horizons (Macrae et al., 2010).

During larger flood events (larger than ~2 year ARI), antecedent soil moisture from the previous storms could retain within the forest area more than in the non-forest area. This is according to the physical characteristics of the forest area which has deeper rote zone and higher soil moisture holding ability, compared to the non-forest area. With the same amount of rainfall occurring at the current flood event, more runoff would be expected in the forest area than that of in the non-forest area. Under these circumstances, runoff coefficient for the forest area would therefore be higher than that of the non-forest area. Once the forest area increases, higher runoff coefficient can be expected (as shown in Table 5 and Figs. 6 and 7). On the other hand, when the non-forest area increases, lower runoff coefficient would be expected.

Table 6
Correlations of runoff coefficients (C) and land cover for smaller flood events for selected sub-catchments in the UPRB.

Runoff station	$C = a + b\ (F)$			$C = a + b\ (DF + Ag)$		
	a	b	r	a	b	r
P.4A	0.366	−0.0034	0.48	0.034	0.0030	0.43
P.14	0.160	−0.0014	0.49	0.017	0.0016	0.52
P.20	0.579	−0.0057	0.53	−0.003	0.0079	0.59
P.21	0.344	−0.0026	0.56	0.082	0.0032	0.58
P.24A	0.300	−0.0023	0.54	0.077	0.0024	0.51
P.42	0.191	−0.0017	0.42	0.013	0.0018	0.42
P.64	0.623	−0.0038	0.57	0.232	0.0039	0.57
P.65	1.303	−0.0126	0.54	0.035	0.0127	0.54
P.71	0.198	−0.0018	0.56	0.016	0.0017	0.56
P.76	0.234	−0.0017	0.43	0.070	0.0018	0.26
P.77	0.325	−0.0027	0.47	0.050	0.0031	0.47
Average			0.51			0.50

5.3. Correlations between runoff coefficients and land cover for smaller flood events

Moderately strong linear correlations between runoff coefficients and forest area (F) for individual sub-catchments under flow conditions were found as shown in Table 6. The coefficient of correlation (r) varied between 0.42 and 0.57 across the sub-catchments with an average of around 0.51. The values of parameter (b) of each sub-catchment varied between −0.0126 and −0.0014, while parameter (a) significantly varied between 0.160 and 1.303.

Similarly good linear correlations were found between runoff coefficients and disturbed forest plus agricultural area ($DF + Ag$), the r coefficient varied between 0.26 and 0.59 with an average of around 0.50. However, the values of the parameters were the opposite of the value of parameter (b) on each sub-catchment varying between 0.0016 and 0.0127, while parameter (a) significantly varied between −0.003 and 0.232. Two examples plotted are shown in Fig. 8.

The result for all stations for the smaller flood events is the opposite of the results in the previous section which considered only larger flood events. During smaller flood events (lower than ~2 year ARI), antecedent soil moisture of the catchment is still low, so losses from smaller rainfall events are relatively high. Under these circumstances, rainfall loss rate in the forest catchment is higher than that of the non-forest catchment due to higher evapotranspiration and soil moisture capacity. This is due to the forest soils containing larger pores and fewer intermediate-size pores than the non-forest soils, forest soils, therefore having higher water content than the non-forest soils (Hayashi et al., 2006). With the same amount of rainfall, less runoff would therefore be expected in the forest area than that of in the non-forest area. Runoff coefficients for the forest area would therefore be lower than that of the non-forest area. When the forest area increases, lower runoff coefficient is expected (as shown in Table 6 and Fig. 8). By contrast, once the non-forest area increases, higher runoff coefficient is expected.

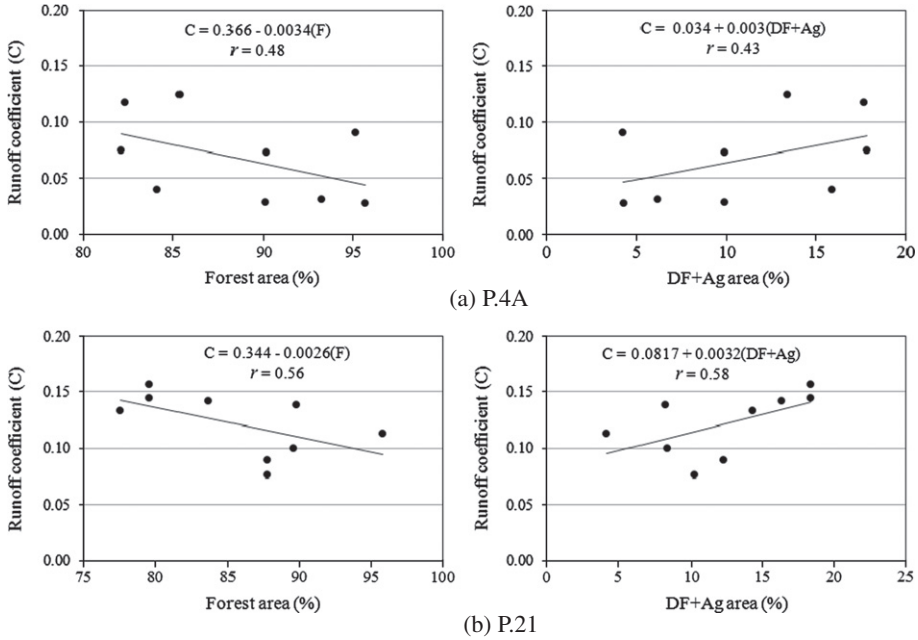

Fig. 8. Typical relationships between runoff coefficients and land cover for smaller flood events of P.4A and P.21 sub-catchments.

6. Summary and conclusions

The type of land cover has been shown to have a significant impact on the runoff generation in many parts of the world (Mahe et al., 2004). In this study, we investigated the effects of land cover on runoff coefficient, which is widely used as a diagnostic variable to represent runoff generation in a catchment. Eleven runoff stations, with the catchment areas ranging between 240 and 3853 km^2, distributed all over the UPRB, were used for the analysis. Land cover types for the catchment area of these stations were classified using nine images of Landsat 5 TM data over the period 1988–2005. First, runoff coefficients and peak flows at each runoff station within the same period were correlated and have shown strong non-linear relationships. This is due to the runoff coefficient being positively correlated with antecedent soil moisture, and in general runoff coefficient increases throughout successive events as the catchment becomes wetter (Macrae et al., 2010). However, at each runoff station, the regression relationships between runoff coefficients and peak flows were different from 1 year to the next. For each regression relationship of each year, we can estimate the runoff coefficients at the 2, 5, 10 and 15 year ARI flood events to correlate with the percentage of forest areas as well as to the summation percentage of the disturbed forest and the agricultural area for each year. Since antecedent soil moisture condition has shown different characteristics between smaller flood (lower than ~2 year ARI) and larger flood events (larger than ~2 year ARI), we separated the analysis between smaller and larger flood events.

For smaller flood events, runoff coefficient in the forest area was found to be lower than that of the non-forest area (disturbed forest and agricultural area) for the same amount of rainfall. This is due to higher evapotranspiration and soil moisture capacity in the forest area compared with the non-forest area. The results show that for the smaller flood events, forest area tends to produce less runoff than the non-forest area. Forests therefore offer flood mitigation benefits for more frequent flood events (Bathurst et al., 2011).

For larger flood events, the situation of the basin can be different, particularly on a basin with high antecedent soil moisture or even close to its saturation stage. Antecedent soil moisture from the previous storms could be better retained within the forest area than the non-forest area. This is because the forest area has deeper rote zone and higher soil moisture holding ability compared to the non-forest area. With high antecedent soil moisture from the previous storm, forest area would need less water than non-forest area to reach its soil saturation stage. Under these circumstances, runoff coefficient in the forest area was therefore found to be higher than that of the non-forest area. When the forest area increased, higher runoff coefficient was found in this study. Once the non-forest area increases, lower runoff coefficient was found.

The insights gained in this study would provide more evidence alongside many other studies which suggest that forests may reduce floods as a result of small to moderate storms but this effect is increasingly reduced as rainfall increases to more extreme levels (Beschta et al., 2000; Sikka et al., 2003; López-Moreno et al., 2006; Bathurst et al., 2011), or forests bring even more flooding once soil moisture of the catchment reach or nearly reach their saturation stage, as we found in this study. The results presented in this study may be a bit counter intuitive, but those are the findings. These findings help us to understand the response of flood behaviour to different land covers within the basin at different stages of antecedent soil moisture and severity of storm events, and can be useful for land use and flood management of the river basin. However, it should be noted that runoff coefficient is also related to other factors such as topography, soil type, and geology. Even though this study actually investigated the correlation between runoff coefficient and land cover types on their own catchments which have the same topography, soil type, and geology, further study on the correlation between runoff coefficient and other factors are recommended.

Acknowledgements

Financial support from the Kasetsart University Research and Development Institute (KURDI) is gratefully acknowledged. The authors are also grateful to the Geo-Informatics and Space Technology Development Agency (GISTDA) for providing all of the Landsat 5 TM images, the Department of Water Resources, the Royal Irrigation Department and Thai Meteorology Department for Providing rainfall and flow rate data. Finally, the authors would like to thank Dr. Michael Waters for editing the manuscript, and also to the anonymous reviewers whose suggestions have helped enhance the paper.

References

Adamson, 2005. Overview of the Hydrology of the Mekong Basin. Mekong River Commission, Vientiane, Lao PDR.
Andréassian, V., 2004. Water and forests: from historical controversy to scientific debate. J. Hydrol. 29, 1–27.
Austin, S.A., 1999. Streamflow response to forest management: a meta-analysis using published data and flow duration curves. Unpublished M.Sc. Thesis. Colorado State University, Fort Collins, CO, USA.
Bates, C.G., Henry, A.J., 1928. Forest and streamflow experiment at Wagon Wheel Gap, Colorado. Monthly Weather Rev. Suppl. 30, 1–79.
Bathurst, J.C., Birkinshaw, S.J., Cisneros, F., Fallas, J., Iroume, A., Iturraspe, R., Novillo, M.G., Urciuolo, A., Alvarado, A., Coello, C., Huber, A., Miranda, M., Ramirez, M., Sarandon, R., 2011. Forest impact on floods due to extreme rainfall and snowmelt in four latin american environments 2: model analysis. J. Hydrol. 400, 292–304.
Beschta, R.L., Pyles, M.R., Skaugset, A.E., Surfleet, C.G., 2000. Peakflow responses to forest practices in the western Cascades of Oregon, USA. J. Hydrol. 233, 102–120.
Bosch, J.M., Hewlett, J.D., 1982. A review of catchment experiments to determine the effect of vegetation changes on water yield and evapotranspiration. J. Hydrol. 55, 3–23.
Bradshaw, C.J.A., Sodi, N.S., Peh, K.S.H., Brook, B.W., 2007. Global evidence that deforestation amplifies flood risk and severity in the developing world. Global Change Biol. 13, 2379–2395.
Buttle, J.M., Metcalfe, R.A., 2000. Boreal forest disturbance and streamflow response, Northeastern Ontario. Can. J. Fish. Aquat. Sci. 57 (Suppl. 2), 5–18.
Buttle, J.M., Lister, S.W., Hill, A.R., 2001. Controls on runoff components on a forested slope and implications for N transport. Hydrol. Process. 15, 1065–1070.
Calder, I.R., Aylward, B., 2006. Forest and floods: moving to an evidence-based approach to watershed and integrated flood management. Water Int. 31 (1).
Chander, G., Markham, B., 2003. Revised Landsat-5 TM radiometric calibration procedures and postcalibration dynamic ranges. IEEE Trans. Geosci. Remote Sens. 41 (11), 2674–2677.
Chander, G., Markham, B., Barsi, J.A., 2007. Revised Landsat-5 thematic mapper radiometric calibration. IEEE Geosci. Remote Sens. Lett. 4 (3), 490–494.
Cosandey, C., Andréassian, V., Martin, C., Didon-Lescot, J.F., Lavabre, J., Folton, N., Mathys, N., Richard, D., 2005. The hydrological impact of the mediterranean forest: a review of French research. J. Hydrol. 301, 235–249.
Department of Disaster Prevention and Mitigation, 2005. Typhoon Damrey Damage Summary. <http://www.dmr.go.th/ewt_news.php?nid=5247&filename=news_dmr>.
Dyhr-Nielsen, M., 1986. Hydrological effect of deforestation in the Chao Phraya basin in Thailand. In: Proceedings of the International Symposium on Tropical Forest Hydrology and Application, Chiangmai, Thailand, 12 pp.
Fraser, R.S., Bahethi, O.P., Al-Abbas, A.H., 1977. The effect of the atmosphere on the classification of satellite observation to identify surface features. Remote Sens. Environ. 6, 229–249.
Fritsch, J.-M., 1990. Les effets du défrichement de la forêt amazonienne et de la mise en culture sur l'hydrologie des petits bassins versants. PhD Thesis. Université des Sciences et Techniques du Languedoc, Montpellier, 392 pp.
Hayashi, Y., Keńichirou, K., Mizuyama, T., 2006. Changes in pore size distribution and hydraulic properties of forest soil resulting from structural development. J. Hydrol. 331, 85–102.
Hewlett, J.D., 1982. Forests and floods in the light of recent investigation. In: Fredericton, N.B. (Ed.), Proceedings, Canadian Hydrology Symposium 82. National Research Council of Canada, Ottawa, Canada, pp. 543–559.
Hibbert, A.R., 1967. Forest treatment effects on water yield. In: Sopper, W.E., Lull, H.W. (Eds.), Forest Hydrology, Proceedings of a National Science Foundation Advanced Science Seminar. Pergamon Press, Oxford, pp. 527–543.
Hornbeck, J.W., Martin, C.W., Eagar, C., 1997. Summary of water yield experiments at Hubbard Brook Experimental Forest, New Hampshire. Can. J. For. Res. 27,

2043–2052.
Kawata, Y., Ohtani, A., Kusaka, T., Ueno, S., 1990. Classification accuracy for the MOS-1 MESSR data before and after the atmospheric correction. IEEE Trans. Geosci. Remote Sens. 28, 755–760.
Kung, K.J.-S., Kladivko, E.J., Gish, T.J., Steenhuis, T.S., Bubenzer, G., Helling, C.S., 2000. Quantifying preferential flow by breakthrough of sequentially applied tracers. Soil Sci. Soc. Am. J. 64, 1296–1304.
Lavabre, J., Sempere Torres, D., Cernesson, F., 1993. Changes in the hydrological response of a small Mediterranean basin a year after a wildfire. J. Hydrol. 142, 273–299.
Legesse, D., Vallet-Coulomb, C., Gasse, F., 2003. Hydrological response of a catchment to climate and land use changes in Tropical Africa: case study South Central Ethiopia. J. Hydrol. 275, 67–85.
Lin, Y., Wei, X., 2008. The impact of large-scale forest harvesting on hydrology in the Willow watershed of Central British Columbia. J. Hydrol. 359, 141–149.
López-Moreno, J.I., Beguería, S., García-Ruiz, J.M., 2006. Trends in high flows in the central Spanish Pyrenees: response to climatic factors or to land-use change? Hydrol. Sci. J. 51 (6), 1039–1050.
Lull, H.W., Reinhart, K.G., 1972. Forests and floods in the Eastern United States. United States Department of Agriculture, Forest Service Research Paper, NE-226.
Macrae, M.L., English, M.C., Schiff, S.L., Stone, M., 2010. Influence of antecedent hydrologic conditions on patterns of hydrochemical export from a first-order agricultural watershed in Southern Ontario, Canada. J. Hydrol. 389, 101–110.
Mahe, G., Paturela, J.E., Servatb, E., Conwayc, D., Dezetter, A., 2004. The impact of land use change on soil water holding capacity and river flow modelling in the Nakambe River, Burkina-Faso. J. Hydrol. 300, 33–43.
McGuinness, J.L., Harrold, L., 1971. Reforestation influences on small watershed streamflow. Water Resour. Res. 7 (4), 845–852.
Merz, R., Blöschl, G., Parajka, J., 2006. Spatio-temporal variability of event runoff coefficients. J. Hydrol. 331, 591–604.
Potter, J.F., 1974. Haze and sun angle effects on automatic classification of satellite data-simulation and correction. Proc. Soc. Photo-Opt. Instrum. Eng. 51, 73–83.
Robinson, M., Gannon, B., Schuch, M., 1991. A comparison of the hydrology of moorland under natural conditions, agricultural use and forestry. J. Hydrol. Sci. 36 (6), 565–577.
Royal Forest Department, 2006. Table 2 – Forest Land Assessment by Province in 2004–2006. <http://www.forest.go.th/stat/stat50/TAB2.htm> (03. 11. 08).
Scepan, J., Menz, G., Hansen, M.C., 1999. The DISCover validation image interpretation process. Photogramm. Eng. Remote Sens. 65 (9), 1075–1081.
Sikka, A.K., Samra, J.S., Sharda, V.N., Samraj, P., Lakshmanan, V., 2003. Low flow and high flow responses to converting natural grassland into bluegum (*Eucalyptus globulus*) in Nilgiris watersheds of South India. J. Hydrol. 270, 12–26.
Song, C., Woodcock, C.E., Seto, K.C., Lenney, M.P., Macomber, S.A., 2001. Classification and change detection using Landsat TM data: when and how to correct atmospheric effects? Remote Sens. Environ. 75, 230–244.
Sriwongsiatnon, N., Surakit, K., Thianpopirug, S., 2011. Influence of atmospheric correction and number of sampling points on the accuracy of water clarity assessment using remote sensing application. J. Hydrol. 401, 203–220.
Taesombat, W., Sriwongsitanon, N., 2009. Areal rainfall estimations using spatial interpolation techniques. Sci. Asia 35 (2009), 268–275.
Taesombat, W., Sriwongsitanon, N., 2010. Flood investigation for the upper Ping river basin using the mathematical models. Kasetsart J. (Nat. Sci.) 44 (1), 152–166.
Troendle, C.A., King, R.M., 1985. The effect of timber harvest on the Fool Creek watershed, 30 years later. Water Resour. Res. 21 (12), 1915–1922.
Uhlenbrook, S., 2006. Catchment hydrology – a science in which all processes are preferential. Hydrol. Process. 20, 3581–3585.
Van Dijk, A.I.J.M., Van Noordwijk, M., Calder, I.R., Bruijnzeel, L.A., Schellekens, J., Chappell, N.A., 2009. Forest–flood relation still tenuous–comment on 'Global evidence that deforestation amplifies flood risk and severity in the developing world' by C.J.A. Bradshaw, N.S. Sodi, K.S.-H. Peh and B.W. Brook. Global Change Biol. 2009 (15), 110–115.
Wei, X., Sun, G., Liu, S., Jiang, H., Zhou, G., Dai, L., 2008. The forest-streamflow relationship in China: a 40-year retrospect. J. Am. Water Resour. Assoc. 44 (5), 1076–1085.
Wilk, J., Andersson, L., Plermkamon, V., 2001. Hydrological impacts of forest conversion to agriculture in a large river basin in northeast Thailand. Hydrol. Process. 15, 2729–2748.